6028 J. Med. Chem. 2010, 53, 6028–6039
DOI: 10.1021/jm100416n

Journal of Medicinal Chemistry Article

Discovery and Mechanistic Study of a Class of Protein Arginine Methylation Inhibitors

You Feng, Mingyong Li, Binghe Wang, and Yujun George Zheng*

Department of Chemistry, Center for Biotechnology and Drug Design, Georgia State University, P.O. Box 4098, Atlanta, Georgia 30302

Received April 2, 2010

Protein arginine methylation regulates multiple biological processes such as chromatin remodeling and RNA splicing. Malfunction of protein arginine methyltransferases (PRMTs) is correlated with many human diseases. Thus, small molecule inhibitors of protein arginine methylation are of great potential for therapeutic development. Herein, we report a type of compound that blocks PRMT1-mediated arginine methylation at micromolar potency through a unique mechanism. Most of the discovered compounds bear naphthalene and sulfonate groups and are structurally different from typical PRMT substrates, for example, histone H4 and glycine- and arginine-rich sequences. To elucidate the molecular basis of inhibition, we conducted a variety of kinetic and biophysical assays. The combined data reveal that this type of naphthyl-sulfo (NS) molecule directly targets the substrates but not PRMTs for the observed inhibition. We also found that suramin effectively inhibited PRMT1 activity. These findings about novel PRMT inhibitors and their unique inhibition mechanism provide a new way for chemical regulation of protein arginine methylation.

Introduction

Among different post-translational modifications, arginine methylation is catalyzed by protein arginine methyltransferases (PRMTs),[a] which utilize the cofactor *S*-adenosyl-L-methionine (AdoMet, SAM) as a methyl donor (Figure 1). Thus far, 11 PRMT members have been identified and are categorized into two major types, type I and type II, according to the substrate and product specificity.[1−3] Type I enzymes (e.g., PRMT-1, -2, -3, -4, -6, and -8) catalyze the transfer of the methyl group from AdoMet to one of the terminal nitrogen atoms of the guanidino group of specific arginine residues in a protein substrate, resulting in ω-N^G-monomethylarginine (MMA, L-NMMA) and ω-N^G,N^G-asymmetric dimethylarginine (ADMA) products.[2,4−7] Type II enzymes (e.g., PRMT 5, 7, and 9) catalyze the formation of MMA and ω-N^G,N'^G-symmetric dimethylarginines (SDMA).[7−10] The catalytic properties of PRMT-10 and -11 remain to be characterized. Protein arginine methylation is involved in a broad spectrum of biological processes, including transcriptional activation and repression, mRNA splicing, nuclear−cytoplasmic shuttling, DNA repair, and signal transduction.[11]

In recent years, the significance of PRMTs in human diseases has been been increasingly recognized. As the predominant PRMT member, PRMT1 is likely to be responsible for bulk protein arginine methylation in mammalian cells. Aberrant expression of spliced forms of PRMT1 has been observed in several tumor states, including breast cancer[12,13] and colon cancer.[14,15] Deregulation of the methylation of histone H4 at R3 (a major cellular substrate of PRMT1) is a suggestive marker of prostate cancer.[16] PRMT1 was recently shown to be a component of mixed lineage leukemia (MLL) transcription complex, and the activity of PRMT1 is required for malignant transformation.[17] PRMT4 [better known as coactivator-associated arginine methyltransferase 1 (CARM1)] is overexpressed in both aggressive prostate cancer and breast tumor.[18,19] The type II PRMT member, PRMT5, is recruited to the promoters of tumor suppressor genes such as ST7 and NM23, and its overexpression was observed in a variety of lymphoma and leukemia cells,[1,20] in gastric carcinoma,[21] and in immortalized fibroblast cells.[22] In cardiovascular disorders, PRMT activity is associated with the up-regulation of serum ADMA, which subsequently blocks NO production and causes many cardiovascular implications such as diabetes and hypertension.[23−25] Furthermore, a number of viral proteins have been shown to be substrates of PRMTs, such as the herpes simplex virus 1 nuclear regulatory protein ICP27, the hepatitis C virus protein NS3, the Epstein−Barr virus nuclear antigen 2, adenovirus E1BAP5 and L4-100K, the HIV-1 proteins Rev and Tat, and the nucleocapsid protein.[6,11] Together, these multiple lines of evidence point toward the extensive roles of PRMTs in human pathogenesis and suggest that PRMT inhibitors could be very useful research tools and have pharmacological merits for disease intervention.

Given the essential roles that PRMTs play in normal biology and in disease, quite a few efforts have been invested in developing small molecule PRMT inhibitors both as chemical genetic tools and as therapeutic agents.[26−28] The first type of chemical inhibitors for PRMTs are analogues of the AdoMet cofactor, including *S*-adenosylhomocysteine (SAH), methylthioadenosine, and sinefungin.[27] Because of structural

*To whom correspondence should be addressed. Tel: 404-413-5491. Fax: 404-413-5505. E-mail: yzheng@gsu.edu.

[a] Abbreviations: PRMT, protein arginine *N*-methyltransferase; CARM1, coactivator-associated arginine methyltransferase 1; GAR, glycine- and arginine-rich domain; AdoMet/SAM, *S*-adenosyl-L-methionine; MMA, ω-N^G-monomethylarginine; ADMA, ω-N^G,N^G-asymmetric dimethylarginine; SDMA, ω-N^G,N'^G-symmetric dimethylarginines; SAH, *S*-adenosylhomocysteine; GST, glutathione *S*-transferase; HAT, histone acetyltransferase; NS-1, naphthalene-sulfo derivative 1; MLL, mixed lineage leukemia; SPPS, solid phase peptide synthesis; DTT, dithiothreitol.

 Published on Web 07/28/2010

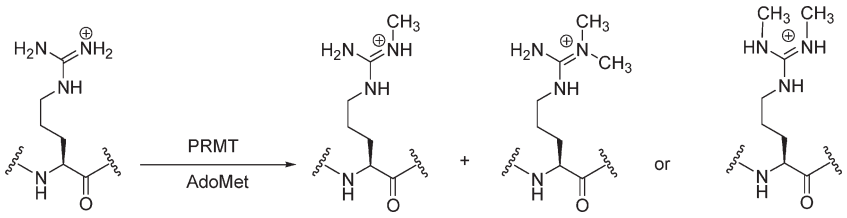

Figure 1. Scheme of protein arginine methylation.

similarities to AdoMet, these analogue inhibitors target all AdoMet-consuming methyltransferases, such as DNA methyltransferases, protein lysine methyltransferases, and *O*-methyltransferases. In the past few years, several groups reported their work in a row on developing small molecule inhibitors specific for PRMTs. Most of these studies on PRMT inhibitor discovery adopted targeted or random screening approaches. The screening strategy is so widely accepted largely because of technical advancement in computer-aided drug design and in medium- and high-throughput inhibitor screening. Thus far, the disclosed small molecule PRMT inhibitors include **1** (AMI-1),[29] stilbamidine and allantodapsone,[30] the thioglycolic amide RM65,[31] pyrazole amide compounds,[32] and others.[33−37] It is important to point out that past inhibitor development efforts were mostly focused on inhibition of the enzyme, presumably, through binding to the active site. This is also the case with the vast majority of enzyme inhibition work reported related to other enzymes so far. Because a single PRMT catalyzes the methylation of arginine residues in multiple proteins, inhibition of a particular PRMT inevitably results in bulky inhibition of methylations of a large number of proteins but not on a particular substrate sequence. Herein, we report our discovery of a class of inhibitors that modulate PRMT-mediated reaction through binding to the substrates, thus revealing a new way of chemical modulation of PRMT activities.

Results

Screening for New PRMT1 Inhibitors. In an effort to discover potent and selective PRMT1 inhibitors, we conducted a virtual screening to search for novel PRMT1 inhibitors from the ChemBridge small molecule compound collection (about 0.4 million compounds) using the reported crystal structure of rat PRMT1.[38] Briefly, the two-dimensional (2D) structures of individual compounds were first converted into three-dimensional (3D) structures by using the CONCORD program[39] and then docked to the PRMT1 structure (PDB entry: 1OR8) using the DOCK 6 program.[40] From this virtual screening, 50 compounds with high consensus scores were selected and experimentally tested for PRMT1 inhibition (see Table SI-1 in the Supporting Information). In a typical radioactive experimental assay, a reaction mixture contained 0.1 μM recombinant His6x-PRMT1, 5 μM [^{14}C]-labeled AdoMet, and 2 μM the amino-terminal tail peptide of histone H4, that is, H4(1−20), as the substrate, and was incubated at 30 °C in the presence or absence of 100 μM individual compounds. The retained fractional activity of PRMT1 was used as a parameter to evaluate the potency of the compounds in blocking PRMT1-mediated methylation. It is notable to mention that, for all of the enzymatic assays, the methylation reaction is maintained under initial conditions so that the reaction yields of the limiting substrates are lower than 10%, which is to ensure that the concentrations of AdoMet and peptide substrate do not decrease significantly over the time course of methylation reaction. The experimental assays, unfortunately, showed that the accuracy of the virtual screening was rather poor. Out of the 50 tested compounds, only one weak hit, **2** (#5252870, ChemBridge product ID), was found to show inhibition potency at an IC_{50} value of about 1 mM. Subsequently, we searched for structural analogues of **2** from the ChemBridge small molecule collection to examine if more potent inhibitors could be found. Thirty-one compounds that bear similar structures or functional groups with **2** were selected, and radioactive methylation assays were performed to evaluate this second set of compounds for inhibition of PRMT1 (Figure 2 and Figure SI-1 in the Supporting Information). From the test, nine compounds were identified to have inhibition activity against PRMT1, and their IC_{50} values ranged from 12 to 867 μM (Table 1). Interestingly, we noticed that some of the tested inhibitors bear great structural similarity to **1**, a previously reported PRMT1 inhibitor by Bedford's group.[29] All of these compounds have rigid, planar, conjugated systems and contain one or more naphthalene aromatic rings. It is also recognized that most of them have negatively charged sulfonate groups and polar hydroxyl groups. Herein, we name these compounds as **3** [naphthalene-sulfo derivative 1 (NS-1)], **4** (NS-2), **5** (NS-3), and so on because of their characteristics of possessing naphthalene and sulfo groups. We also compared the inhibition potencies of these inhibitors with several PRMT1 inhibitors recently reported in the literature, including **1**, stilbamidine, and allantodapsone. As shown in Table 1, stilbamidine (IC_{50} = 105.7 μM) exhibited comparable inhibition activity with **1** (IC_{50} = 137.1 μM). The inhibition potency of the other PRMT1 inhibitors, including allantodapsone and compounds 5756663 and 7280948 reported in the literature,[30,33] is even weaker. For example, at a 2 mM concentration of these three compounds, still 45%, 87%, and 100% of PRMT1 activity retains, respectively. By contrast, the NS series of compounds identified

Table 1. Inhibition of PRMT1 by Selected Compounds[a]

compounds	IC_{50} (μM) for H4(1−20) methylation	IC_{50} (μM) for R4 methylation
3	12.7 ± 0.1	741.7 ± 75.0
4	43.1 ± 1.0	108.4 ± 8.4
5	72.1 ± 1.0	463.1 ± 99.2
6	104.2 ± 3.9	227.8 ± 7.8
7	205.9 ± 25.2	1200 ± 16
8	234.1 ± 10.1	595.8 ± 37.5
9	280.6 ± 27.1	no inhibition at 2 mM
10	325.0 ± 36.9	no inhibition at 2 mM
11	867.4 ± 13.6	no inhibition at 2 mM
stilbamidine	105.7 ± 0.7	1150 ± 33
1	137.1 ± 12.1	375.6 ± 7.8
suramin	5.33 ± 0.23	1011 ± 20

[a] IC_{50} values of different NS compounds were tested in the radioactive inhibition assays with 2 μM H4(1-20) or R4, 5 μM [^{14}C]-AdoMet, 0.1 μM PRMT1, and increasing concentrations of each inhibitor.

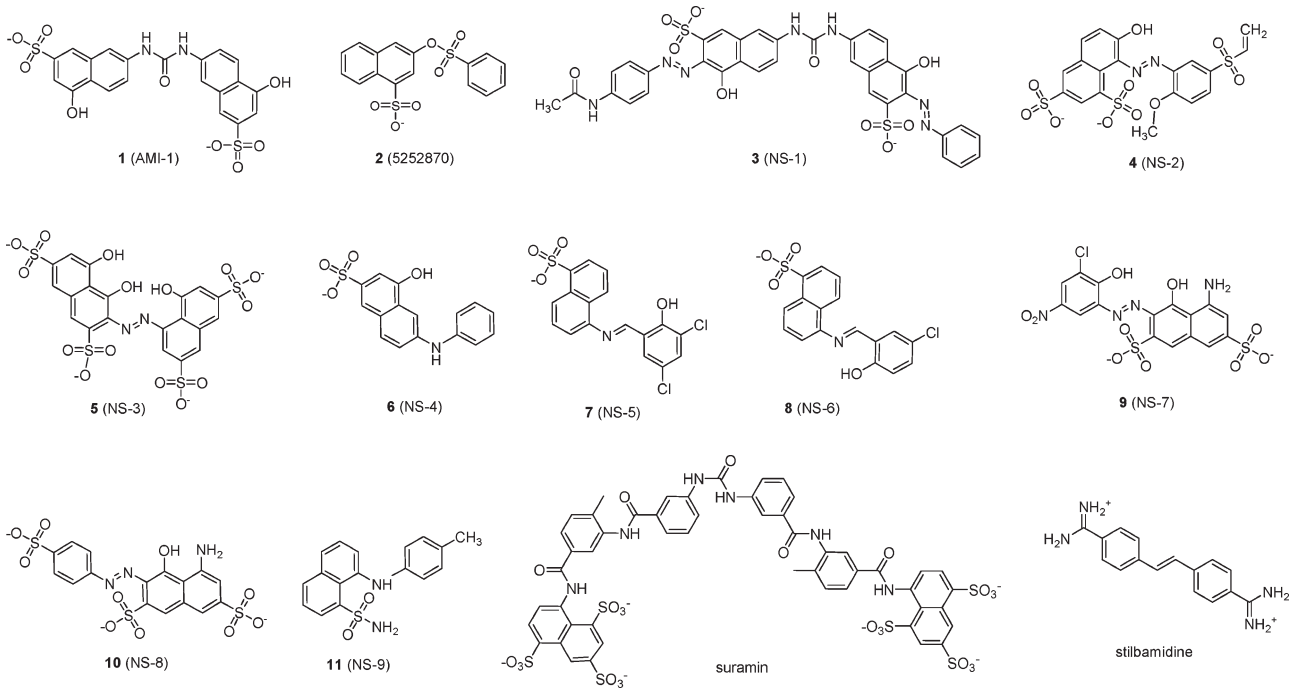

Figure 2. Structures of selected PRMT1 inhibitors.

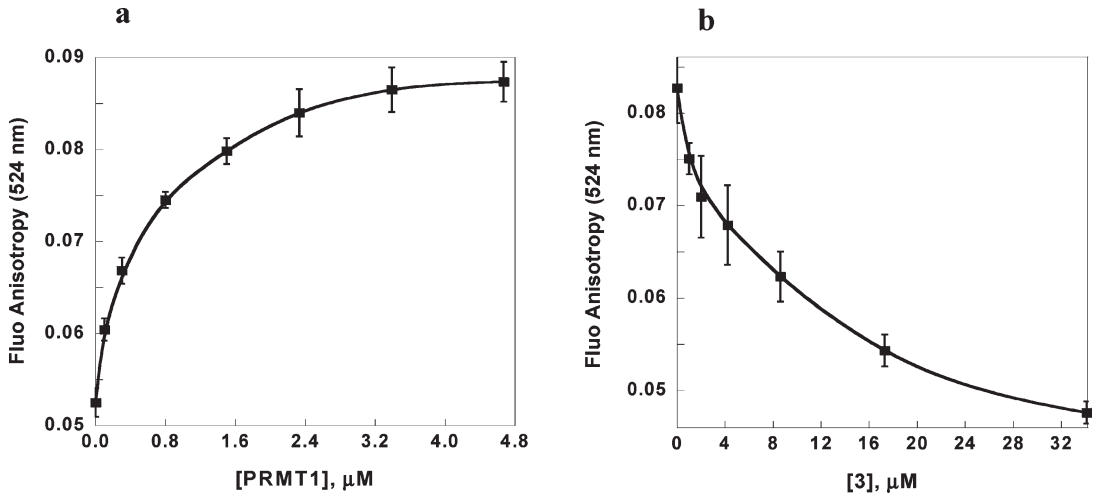

Figure 3. Competitive binding measurement with fluorescence anisotropy. (a) Fluorescence anisotropy of H4(1−20)FL at different concentrations of PRMT1. The concentration of H4(1−20)FL was fixed at 0.2 μM. K_d of H4(1−20)FL to PRMT1 was calculated to be 0.49 ± 0.10 μM. (b) Fluorescence anisotropy (524 nm) of H4(1−20)FL and PRMT1 complex at different concentrations of **3**. The concentrations of H4(1−20)FL and PRMT1 were kept constant at 0.2 and 2.0 μM, respectively. The K_i of **3** was calculated to be 1.71 ± 0.54 μM by fitting the titration data with the DynaFit program.

here are quite stronger PRMT1 inhibitors. Four of these inhibitors, that is, **3**, **4**, **5**, and **6** (NS-4), showed stronger potency than **1** and stilbamidine. In particular, **3** exhibited the best inhibition potency with an IC_{50} value of 12.7 μM, which is about 10-fold lower than that of **1** and stilbamidine under the same reaction conditions.

Kinetic Pattern of PRMT1 Inhibition by 3. To provide the biochemical basis of PRMT inhibition by this type of NS compound, we investigated the inhibition mechanism of **3**, the most potent inhibitor in the series. First, we performed a fluorescence anisotropy binding assay to check if the inhibitor can compete with the PRMT1 substrates. In this experiment, a fluorescein-labeled amino-terminal H4 peptide, namely, H4(1−20)FL, with the sequence of Ac-SGRGKGGKGDpr(FL)GKGGAKRHRK, was used as a substrate ligand for PRMT1 binding.[41] The anisotropy of H4(1−20)FL increased upon binding to PRMT1, due to formation of a large macromolecular PRMT1−ligand complex (Figure 3). A K_d value of 0.49 ± 0.10 μM was calculated. The addition of **3** led to reversal of the anisotropy change, thus offering direct evidence that **3** is a competitive inhibitor versus the peptide substrate. A K_i value of **3** was deduced to be 1.71 ± 0.54 μM by fitting the titration data using the DynaFit program.[42] Similar competitive binding between **3** and a fluorescently labeled glycine- and arginine-rich (GAR) substrate, R4FL, was also observed (Figure SI-2 in the Supporting Information). To further validate the results of competitive inhibition, we conducted steady-state kinetic characterization. The initial velocities of PRMT1 were measured at several selected concentrations of the inhibitor over a range of varied

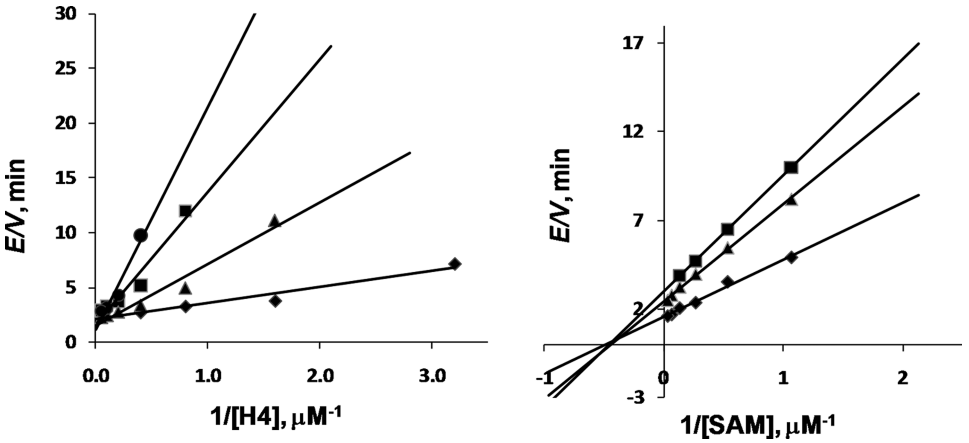

Figure 4. Kinetic analysis of PRMT1 inhibition by **3**. (a) Double-reciprocal plotting of initial velocities vs varied concentrations of H4(1−20). The concentration of [^{14}C]-AdoMet was fixed at 5 μM, and the concentration of **3** was selected at 0 (♦), 5 (▲), 10 (■), and 20 μM (●). (b) Double-reciprocal plotting of initial velocities vs varied concentrations of [^{14}C]-AdoMet. The concentration of H4(1−20) was fixed at 2 μM, and the concentration of **3** was selected at 0 (♦), 5 (■), and 10 μM (▲). A 0.03 μM concentration of His6x-rPRMT1 was used in all of these assays.

concentrations of one substrate while fixing the concentration of the other. The data were plotted in the double reciprocal fromat with 1/velocity versus 1/concentration of the varied substrate (Figure 4). The kinetic inhibition data points were analyzed by fitting to the linear competitive or noncompetitive inhibition equations.[43] As can be seen from the double-reciprocal plots, a series of straight lines intersected on the 1/velocity ordinate when the concentrations of H4(1−20) are varied, while the intersecting point moved to the western side of the ordinate when concentrations of AdoMet are varied. These data clearly demonstrate that **3** is competitive versus the peptide substrate and noncompetitive versus the methyl donor. This result is consistent with the fluorescent binding assay and is also in agreement with our previous report showing that **1** is competitive versus peptide substrates and noncompetitive versus AdoMet.[41] In addition, **6**, another inhibitor in this class, also exhibited the same inhibition pattern (Figures SI-3 and SI-4 in the Supporting Information). These combined results support that these types of naphthalene-sulfo derivatives target PRMT1 by blocking the access of the substrate to the PRMT1 active site. Interestingly, the positively charged stilbamidine also showed a competitive binding pattern with respect to the peptide substrate (Figure SI-4 in the Supporting Information), which is consistent with a previous report.[30]

Selectivity of 3. It is of interest to examine whether the NS inhibitors target PRMT1 selectively or also inhibit other PRMT members. Using radioactive methylation assays, we measured inhibitory activities of **3**, the most potent compound in this series, toward PRMT3, PRMT4/CARM1, and PRMT6 (Table 2). The inhibition potency of **3** for glutathione *S*-transferase (GST)-tagged PRMT1 is similar to that for His6x-PRMT1, with an IC_{50} of 12.9 ± 0.2 μM. PRMT3 was inhibited at a lower IC_{50} at 7.1 μM. At the concentration of 500 μM, **3** showed no apparent inhibitory effect to CARM1 (5 μM CARM1, 1 mM H3(1−31), and 30 μM SAM). The IC_{50} for PRMT6 is about 3-fold larger than that for PRMT1. It is worth mentioning that PRMT1 and PRMT3 share similar substrate specificity, both of which methylate H4 and GAR peptides. On the other hand, CARM1 exhibits distinct substrate specificity from PRMT1. CARM1 targets H3 but does not methylate GAR sequences.[6] Therefore, the variation in inhibition potency is likely caused either by the differences between CARM1 and PRMT1 structures or by the distinct nature of the substrates used. Overall, **3** inhibits PRMT1 and PRMT3 stronger than CARM1 and PRMT6.

Table 2. Comparison of the Inhibition of PRMT-1, -3, -4, and -6 by **3**[a]

	peptide substrate and its K_m (μM)	IC_{50} (μM)
His6x-rPRMT1	H4(1−20); 0.64 ± 0.04	12.7 ± 0.1
GST-hPRMT1	H4(1−20); 0.69 ± 0.04	12.9 ± 0.2
His6x-PRMT3	R4; 0.92 ± 0.15	7.1 ± 0.2
GST-CARM1	H3(1−31); 796 ± 204	~2 mM
His6x-PRMT6	H3(1−31); 9.1 ± 1.2	39.2 ± 2.8

[a] Data obtained from the results of the radioactive methylation assays. For inhibition of His6x-rPRMT1 or GST-hPRMT1, 2 μM H4(1-20), 5 μM [^{14}C]-SAM, and 0.1 μM enzyme were used. For inhibition of His6x-PRMT3, 2 μM R4, 5 μM [^{14}C]-SAM, and 0.1 μM enzyme were used. For inhibition of GST-CARM1, 1 mM H3(1-31), 30 μM [^{14}C]-SAM, and 5 μM enzyme were used. For inhibition of His6x-PRMT6, 10 μM H3(1-31), 5 μM [^{14}C]-SAM, and 0.5 μM enzyme were used.

Compound 3 Directly Targets the Substrates but Not PRMT1. One paradox question is that the NS series of inhibitors bear none or little structural similarity to the arginine-containing substrates of PRMT1 such as histone H4 or GAR peptides. In particular, all of the reported PRMT1 substrates are rich in positive residues, that is, arginines and/or lysines. The crystal structure of PRMT1 also reveals several large acidic grooves present at the protein surface, which have been proposed to participate in the recognition of substrates.[38] On the other hand, most of the NS compounds are negatively charged due to the existence of one or more sulfonate groups. Therefore, it seems difficult to envision that **3** and its analogues will bind to PRMT1 at the same site as that of substrates to explain the competitive nature between the inhibitor and the peptide substrates. To look into these paradox problems, we hypothesized that **3** and its analogue inhibitors might bind to the PRMT1 substrate directly and that the binding subsequently prevents the substrate from accessing to PRMT1. Under this scenario, the inhibitor−substrate interaction is likely facilitated by the electrostatic interaction between the negatively charged sulfonate groups and the cationic arginine guanidino group, as well as the van der Waals interaction between the naphthalene ring and the hydrophobic side chains in the substrate. It is conceivable that such an interaction may shield the key motifs in the substrate so that they are not recognized by enzyme. To nail down the mechanistic details, we conducted

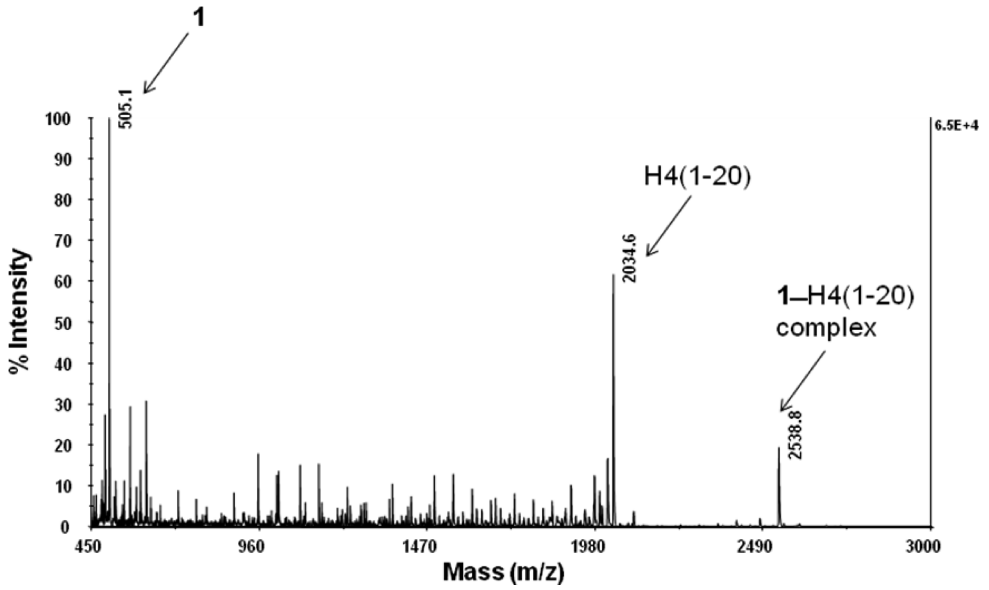

Figure 5. Association of **1** with H4(1−20) peptide detected by MALDI-MS. A 100 μM concentration of H4(1−20) and 200 μM concentration of **1** were mixed in the reaction buffer. The precipitate formed was pelleted by centrifugation, washed with H_2O, dissolved in 5% TFA, and analyzed by MALDI-MS.

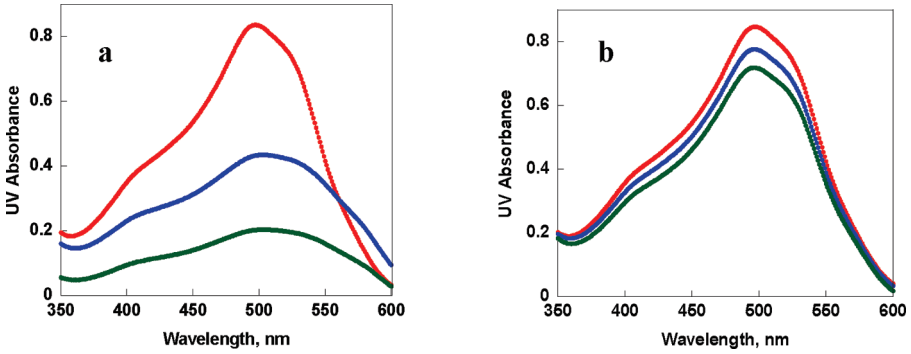

Figure 6. UV−vis spectral change of **3** upon the addition of H4(1−20) or His6x-PRMT1. A 40 μM concentration of **3** was titrated with 0 (red), 5 (blue), and 10 μM (green) H4(1−20) (a) or PRMT1 (b).

several biophysical measurements to detect inhibitor−substrate and inhibitor−enzyme associations.

The interaction between the inhibitors and the PRMT1 substrate was confirmed by several experiments. First, when mixing high concentrations of H4(1−20) and **3** or **1** (e.g., 100 μM peptide and 200 μM inhibitor), a red or brown precipitate occurred immediately. We reasoned that the precipitation is a strong indication of the association between the H4 substrate and the inhibitors. The precipitate was pelleted by centrifugation, washed with water, dissolved in 5% TFA, and analyzed with matrix-assisted laser desorption/ionization mass spectrometry (MALDI-MS). Indeed, the mass spectra revealed a peak corresponding to the H4(1−20)−**1** complex (Figure 5). We could not observe a peak for the H4(1−20)−**3** complex on MS spectra, probably due to the instability of the complex and/or the strong anionic nature of **3**.

Next, we examined UV−vis spectra of **3** in the presence of different concentrations of H4(1−20) or PRMT1 (Figure 6). Compound **3** has a maximum absorption at 498 nm with an extinction coefficient of 0.0182 μM^{-1} cm^{-1}. When H4(1−20) was gradually added to a solution of **3** (the concentration of **3** was kept constant at 40 μM), the absorbance decreased dramatically. For instance, at 10 μM H4(1−20), the absorbance at 498 nm decreased to 25% of the original value. By contrast, the presence of PRMT1 had a quite minor effect on the absorption of **3**. At 10 μM PRMT1, the absorbance of **3** at 498 nm still retained 83%. These data directly pointed out that the interaction between **3** and H4(1−20) is much stronger than the **3**−PRMT1 interaction (if there is any).

We then measured the fluorescence emission of H4(1−20)FL in the presence of **3**. Because the absorption band of **3** overlaps with the fluorescence emission peak of H4(1−20)FL, it is anticipated that fluorescence energy transfer from fluorescein (donor) to the **3** (acceptor) will occur if the two molecules form a complex. Indeed, the addition of the inhibitor quenched the fluorescence emission of H4(1−20)FL (Figure 7). On the other hand, in the control experiment, the addition of the inhibitor to a fluorescein solution caused little change to its fluorescence spectra (after removing the inner filter effect). These data demonstrate that the interaction between the inhibitor and the H4(1−20)FL depends on the H4 peptide itself, instead of being caused by the attached fluorescein label. The K_d of **3** from the fluorescence binding measurement is 2.53 ± 0.64 μM, which is in a similar range as the value measured from the fluorescence anisotropy titration. Furthermore, we determined the binding stoichiometry of **3** with H4(1−20)FL by using Job's method (Figure 8). The

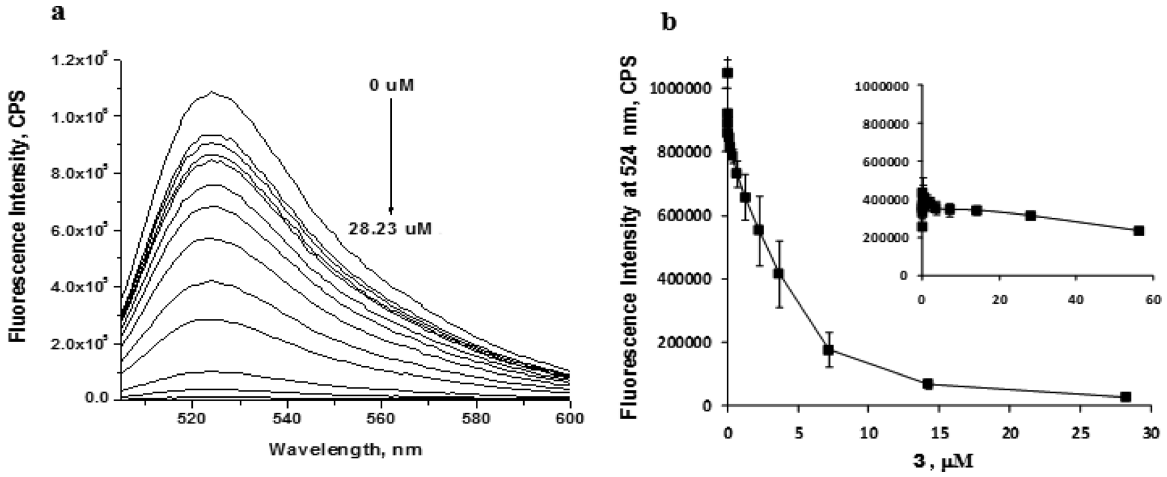

Figure 7. Impact of **3** on the fluorescence spectra of H4(1−20)FL. (a) Fluorescence emission spectra of H4(1−20)FL (0.2 μM) at different concentrations of **3** (0−28.2 μM). The excitation wavelength was 498 nm. The fluorescence spectrum change of NHS-fluorescein (0.2 μM) upon titration with **3** was also measured as a control (spectra not shown). (b) Fluorescence intensity of H4(1−20)FL at 524 nm as a function of **3** concentration (after removing the inner filter effect). Inlet: Fluorescence intensity of NHS-fluorescein at 524 nm as a function of **3** concentration (after correction).

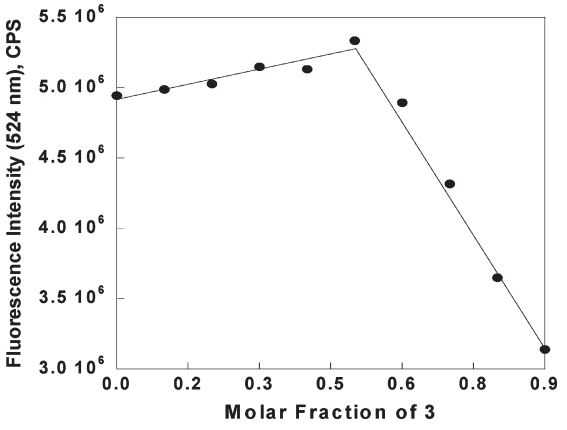

Figure 8. Determination of the binding stoichiometry of **3**−H4-(1−20)FL complex by Job's method. The ratio of **3**/H4(1−20)FL was varied while the total concentration of H4(1−20)FL and **3** was fixed at 0.5 μM. The fluorescence intensity (524 nm) of each solution was measured and normalized and plotted as a function of the molar fraction of **3**.

intersecting point appears at 0.5 in the plot, suggesting that **3** binds to H4(1−20)FL at a 1:1 ratio.

We also attempted to study the **3**−H4(1−20) interaction using circular dichroism (CD) spectra. In the spectra, H4(1−20) showed a pattern of absorption that is correspondent with random coil structures (Figure SI-5 in the Supporting Information). Upon addition of **3**, the absorption band for the random coil decreased, indicating that the inhibitor caused a structural change to the H4 peptide. However, upon continuous addition of **3**, a red precipitate occurred that prevented further accurate quantitative analysis of the H4(1−20)−inhibitor interaction. Similar results were also observed for the interaction between **1** and H4(1−20) (data not shown).

In enzyme inhibition, if an inhibitor targets the active site of an enzyme, its inhibition potency will be largely determined by the binding affinity between the inhibitor and the enzyme, with little interference by substrates. In our case, however, the experimental findings show that NS compounds target the substrate but not the enzyme. This suggests that the potency of these inhibitors in blocking PRMT1 activity will be greatly affected by the nature of the substrate used for the assay. To investigate whether this is true, we tested PRMT1-mediated methylation on H4(1−11) and the inhibition by **3**. Indeed, **3** inhibited the methylation of H4(1−11) with an IC_{50} (i.e., 176.5 μM) significantly higher than that of H4(1−20) methylation (i.e., 12.7 μM). These data indicate that the inhibition caused by the NS molecules depends on the structural sequences of the substrates used and strongly validate the proposal that these inhibitors target substrate instead of enzyme. On the other hand, stilbamidine inhibited the methylation of H4(1−20) and H4(1−11) with similar K_i values, that is, 25.6 and 35.0 μM, respectively. Therefore, the inhibition mode of stilbamidine is different from that of NS compounds. Our data, in agreement with a previous study,[30] support that stilbamidine targets the active site of PRMT1 to compete with substrates.

By now, there is no structural information available regarding the nature of the H4(1−20)−**3** interaction. The potency difference of **3** in inhibiting H4(1−20) methylation versus H4(1−11) methylation suggests that the inhibitor targets both the N-terminal and the C-terminal residues in H4(1−20). The 1:1 stoichiometry of H4(1−20)−**3** binding indicates that the interaction is quite specific. Electrostatic interaction is likely a strong factor, but other modes of interactions such as van der Waals and hydrogen bonding may also play significant roles. On the basis of the results of CD, fluorescence, and absorption spectral changes, it is quite possible that the secondary structure of the peptide substrate is altered upon inhibitor binding.

Compound 3 Inhibits the Activity of Histone Acetyltransferase (HAT) p300. The finding that **3** and its analogues inhibit PRMT1 activity by targeting its substrates implicates that **3** may also inhibit other enzymes that utilize H4 or GAR peptides as substrate. To test this possibility, we measured the acetylation of H4(1−20) by p300, a well-known HAT that is able to acetylate the N-terminal tail of H4 at multiple sites.[44] The measurement was carried out with 0.02 μM p300, 10 μM [^{14}C]-acetyl CoA, and 10 μM H4(1−20), at varied concentrations of **3** or **1**. Indeed, both compounds exhibited strong inhibition of p300-mediated H4 acetylation (Figure 9). The IC_{50} values of **3** and **1** for p300 inhibition were determined

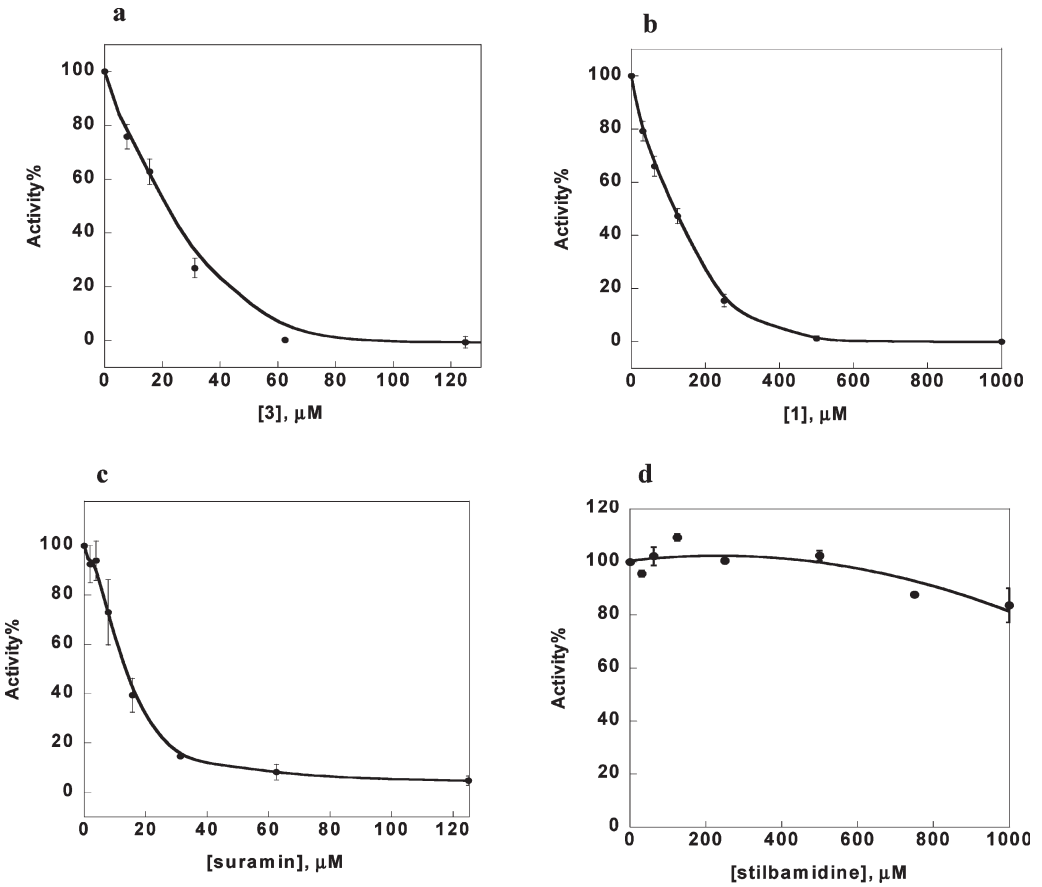

Figure 9. Inhibition of p300 HAT activity by **3**, **1**, suramin, and stilbamidine. The fractional activity of p300 was plotted with respect to the concentration of **3** (a), **1** (b), suramin (c), or stilbamidine (d). The reaction buffers contained 10 μM H4(1−20), 10 μM ^{14}C-Acetyl CoA, and 20 nM p300.

to be 21.3 ± 2.0 and 118.5 ± 6.5 μM, respectively. Notably, these IC_{50} values are very similar to those obtained for PRMT1 inhibition. These data again support our conclusion that the NS series of compounds binds to H4 directly, and the binding subsequently prevents H4 from being recognized by the H4-modifying enzymes, such as PRMT1 and p300. Thus, the inhibition caused by NS series compounds depends on the binding between the inhibitor and the substrate, irrespective of enzyme targets. On the other hand, although stilbamidine is a competitive inhibitor in PRMT1-catalyzed methylation, it does not inhibit significantly H4 acetylation catalyzed by p300 (Figure 9d). For example, at 1 mM stilbamidine concentration, p300 still retained 84% of its HAT activity. Therefore, quite likely, stilbamidine targets the active site of PRMT1 to compete with the H4 substrate, which is in agreement with a previous study.[30]

Suramin Inhibits Arginine Methylation. The NS series of compounds has great structural similarity to suramin, a symmetrical polyanionic aromatic urea containing two naphthalene and six sulfonate groups (Figure 1). We tested whether suramin could inhibit PRMT1-mediated methylation. Indeed, suramin strongly inhibited arginine methylation on both H4(1−20) and GAR substrate R4, with IC_{50} values of 5.3 and 1011 μM, respectively (Table 1). As a matter of fact, the inhibition potency of suramin is even stronger than that of **3**, the most potent inhibitor identified from our screening search. Furthermore, suramin also inhibited the HAT activity of p300 with an IC_{50} value of 13.7 μM (Figure 9c). Given their structural analogy and the similar properties in the inhibition of methylation and acetylation, suramin likely shares the same mechanism of inhibition with NS compounds, namely, suramin also targets H4 and GAR proteins and blocks PTMs on the substrates. These data revealed a previously unknown function of sumarin.

Discussion

The development of PRMT inhibitors represents an active research endeavor in the field of epigenetics. Because PRMT-mediated arginine methylation regulates nucleosomal remodeling, gene expression, DNA repair, RNA processing and shuttling, and other cellular processes, PRMT inhibitors will be useful tools to dissect the function of protein arginine methylation and the pathways in which PRMTs participate. In this work, we initially attempted to discover PRMT1 inhibitors by using the approach of virtual screening to dock individual small molecules from the ChemBridge compound collection to the crystal structure of rat PRMT1, but the experimental tests only yielded one millimolar-potent inhibitor (i.e., **2**) out of the 50 compounds that were predicted from the virtual screening. The reason for such a low efficiency of virtual screening is not clear at this time. One possible reason might be that the structure of PRMT1 used in the virtual screening was obtained under nonphysiological conditions (pH 4.7) and the structural conformation of PRMT1 may be different from that at pH 8.0 under which the biochemical assays were carried out. In this respect, better success rates have been observed by Jung and co-workers who performed

virtual screening of PRMT1 inhibitors using homology hPRMT1 and *A. nidulans* RmtA models that were generated on the basis of the rat PRMT3 X-ray structure, which was more physiologically relevant.[30,33]

By searching and testing structural analogues of the weak hit **2**, we identified several naphthalene-sulfo-containing PRMT1 inhibitors with potency in the micromolar range. Four of them, that is, **3**, **4**, **5**, and **6**, exhibited stronger potency than **1** and stilbamidine, two effective PRMT1 inhibitors reported previously. Compound **3** has the strongest potency, with an IC_{50} value of 12.7 μM in our assay using H4(1−20) as a substrate. It is notable that the IC_{50} values of inhibitors may vary depending on different experimental conditions used. For instance, the IC_{50} values of **1** and stilbamidine were measured to be 1.2 ± 0.5 and 56.9 ± 6.2 μM, respectively, in a previous study.[30] In our inhibition assays, these values were determined as 137.1 ± 12.1 and 105.7 ± 0.7 μM (Table 1). The differences reflected the influence of assay conditions used. It is well-known that IC_{50} is a relative parameter for the evaluation of the inhibition potency of enzyme inhibitors, and its quantitative value can be affected dramatically by experimental parameters such as assay formats, signal readouts, enzyme resources, the nature and concentration of substrates, reaction time, temperature, etc. It is worth pointing out that all of our measurements were carried out using simple radioactive methylation assays or fluorescent binding tests. The enzymatic processes were analyzed under initial condition so that the change of substrate concentrations and the effect of product inhibition were negligible.

Our fluorescence binding and enzymatic methylation data showed that the tested NS compounds inhibited PRMT activity in a competitive manner against the peptide substrates, that is, H4(1−20) and the GAR peptide R4. This result is in agreement with our previous report showing that **1** competes with peptides but not with AdoMet in PRMT1 inhibition.[41] Importantly, our experimental data, which include steady-state kinetics, fluorescence anisotropy and intensity titrations, MS, and UV−vis, strongly support that these NS compounds directly target the substrates but not the enzyme to achieve the observed competitive inhibition effect. Because the structures of the tested inhibitors all contain naphthalene and sulfonyl groups, these two motifs likely are the key components of the pharmacophores for this type of PRMT inhibitors. Our data showed that **3** and **1** inhibited the activity of PRMT1 regardless of H4(1−20) or R4 being used as substrates but with different potencies. This provides additional evidence supporting that these compounds target PRMT1 substrates, instead of the enzyme. The result is also in accord with a previous study showing that the methylation of Npl3, a protein rich in GAR motifs, was inhibited by **1**.[29]

In our experiment, it was noted that with the same H3(1−31) peptide substrate, PRMT6 was inhibited to a larger degree than CARM1 in the presence of **3**. Given that PRMT6 methylates R2 while CARM1 predominately methylates R17 of H3, it is likely that the difference in inhibition potency is related to the substrate site specificity of the two PRMT members; namely, **3** targets the amino acid residues that are adjacent to arginine 2 but relatively distal from arginine 17 in the substrate H3(1−31). In addition to histones, PRMT1 methylates a variety of proteins at GAR regions. In our experiments, we designed a typical GAR peptide, R4, and tested its methylation by PRMT1 as well as inhibition by the NS series of inhibitors. From Table 1, it can be seen that the inhibition potency of NS compounds toward GAR peptide methylation is generally weaker than that of H4 methylation. The difference in inhibition potency caused by substrates further supports the proposal that the naphthalene-sulfo molecules target substrates but not enzymes for inhibition. The weaker potency of NS compounds in inhibiting R4 methylation is likely because multiple methylating arginine residues exist in the R4 sequence and binding of an inhibitor is not sufficient to block the methylation at the other sites. Thus far, no structural information is available about the molecular basis of NS−substrate interactions. It is possible that the anionic sulfonate substituents create electrostatic and hydrogen-bonding interactions with the guanidino nitrogens of the target arginine residues in PRMT1 substrates, and the naphthalene ring interacts with the arginine side chain through π-stacking and van der Waals contact. The other functional moieties of the inhibitors may fine-tune and further enhance the inhibition by interacting with peptide backbones and other residues in the substrates. It is worth noting that the inhibitor−substrate assoication seems quite specific and is not exclusively determined by electrostatic factors. For example, **9** (NS-7) and **10** (NS-8) contain two and three sulfonates, but their inhibition potencies are weaker than those of **6**, which contains only one sulfonate group. The Job's plot shows that **3** binds to H4(1−20)FL with a clear 1:1 stoichiometry, suggesting that the binding is quite specific. An effort is in progress to obtain cocrystal structures of **3** with H4(1−20) and GAR peptides. On the other hand, although demonstrated to inhibit PRMT1-mediated H4 methylation, stilbamidine did not inhibit H4 acetylation catalyzed by p300. These distinct inhibitory properties suggest that the molecular basis of stilbamidine for PRMT1 inhibition differs from that of **3** and **1**; that is to say, stilbamidine directly targets the active site of PRMT1, but the NS series of compounds targets the substrates of PRMT1. From a structural point of view, the competitive nature of stilbamidine and PRMT1 substrates seems reasonable because the cationic formamidine group in stilbamidine is analogous to the guanidino group in arginine residues.

The mechanism by which the NS series of inhibitors (including **1**) target the substrates rather than PRMT implicates that they may have unique applications in comparison to classic enzyme-targeting inhibitors. Previously, **1** has been shown in cellular assays to block PRMT1-mediated protein methylation and transactivation of luciferase reporter genes.[29] Because the N-terminal tail of H4 undergoes a variety of post-translational modifications, for example, phosphorylation at the S1 site,[45,46] arginine methylation at the R3 site,[47] lysine acetylation at the K5, K8, K12, and K16,[48−52] and lysine methylation at the K20 site, etc.,[53−55] it is conceivable that the binding of the amino-terminal tail of H4 to **3**, **1**, or other NS series of compounds will influence many modifications occurring on the N-terminal tail of H4 in addition to arginine methylation, although the degree of influence on individual modifications may vary. Our data about the inhibition of p300-catalyzed H4 acetylation by both **3** and **1** clearly substantiate this potential. Interestingly, during the preparation of this paper, we noticed that Kundu and co-workers reported that TBBD (ellagic acid), a chemical component from the pomegranate extract, inhibited methyltransferase activity of PRMT4/CARM1 also in the substrate-targeting manner.[56] TBBD was determined to target histone H3 near the arginine 17 site and has been used to elucidate the significance of H3R17 methylation in the p53-responsive gene expression pathway.

Organic compounds that contain naphthyl and sulfonate groups have been previously reported to have multiple biological

impacts. For example, **1** and several analogue molecules that contain naphthyl, urea, and sulfonate groups were shown to inhibit the activity of HIV-1 reverse transcriptase (RT) by preventing the binding of DNA substrates to the enzyme, and structural similarities of those compounds to DNA base pairs were also conjectured therein.[57] Suramin, a symmetrical polyanionic aromatic urea, also contains naphthalene-sulfonate groups. Suramin is an antiparasitic drug but also showed efficacy for the treatment of several kinds of carcinomas.[58,59] Biochemically, suramin binds to and inhibits a variety of enzymes (e.g., thrombin,[60] vaccinia virus complement control protein,[61] and NAD^+-dependent deacetylase SIRT5[62]) and peptidic growth factors (e.g., epidermal growth factor[63] and fibroblast growth factor[64]) (see ref 58 for a recent review). Our data clearly showed that suramin inhibits the activity of PRMT1 on both H4 and GAR substrates, thus disclosing a possible new biological function of suramin and its derivatives. Also, it would be intriguing to investigate whether the NS series of compounds studied here also have similarly broad biological effects.

One minor concern is that the NS compounds are negatively charged and may have low membrane permeability. This could limit their biological applications for PRMT functional study. It will be necessary to investigate how efficiently these NS compounds cross plasma membranes. Nevertheless, it is of note that many anionic compounds, such as **1** (a structural analogue in the NS series),[29] ellagic acid,[56] and anarcardic acid,[65] have been shown to be cell permeable and have intracellular inhibition activities. Also, the issue of cell permeability could be improved by adding drug delivery vehicles or chemically modifying the compounds in pro-drug formats. In addition to in vivo applications, the NS inhibitors are valuable chemical probes for the mechanistic study of PRMTs and other histone-modifying enzymes in biochemical systems. For instance, they can be used to investigate substrate−enzyme interactions and downstream effector modules that recognize arginine methylation marks in histones.

Conclusion

In conclusion, we have discovered a type of organic compounds containing naphthalene and sulfonyl pharmacophore components that inhibit PRMT activity in the micromolar range, whose inhibition mechanism is fundamentally distinct from the other PRMT inhibitors reported so far. The biochemical and biophysical data of representative compounds (e.g., **3**, **6**, and **1**) show that these inhibitors are competitive versus PRMT1 substrates (e.g., H4 and GAR peptides) and noncompetitive versus the methyl donor. Detailed studies illustrate that they directly target the peptide substrates instead of PRMT1, and the binding subsequently blocks the recognition of the substrates by enzyme, which is largely responsible for the observed PRMT1 inhibition effect. We also show that the antiparasitic drug suramin is also an effective arginine methylation inhibitor. These NS inhibitors will be useful chemical tools for the mechanistic study of arginine methylation and other epigenetic modifications. Furthermore, illumination of the inhibitory mechanism provides a new insight for understanding the pharmacological effect of these structurally unique molecules in biological systems.

Experimental Section

Materials. Fmoc-protected amino acids and solid phase resins were purchased from NovaBiochem. All of the screening compounds were obtained from ChemBridge Corp. Stilbamidine and allantodapsone were obtained from the National Cancer Institute. Suramin was purchased from Acros Organics. For all of the effective inhibitors discovered and tested, including compounds **1**, **3**−**11**, suramin, and stilbamidine, their purities were confirmed to be ≥95% by analytical C18 reverse-phased high-performance liquid chromatography (HPLC). Radioactive AdoMet and acetyl-CoA were ordered from GE Healthcare and Perkin-Elmer. Other chemical reagents were purchased from Fisher, VWR, and Sigma, etc.

Peptide Substrates. Peptides were synthesized using the standard solid phase peptide synthesis (SPPS) protocols, purified with C-18 reversed phase HPLC, and confirmed with MALDI-MS as previously described.[66] The sequence of the NH_2-terminal 20 aa peptide of histone H4, H4(1−20), is Ac-SGRGKGGKGLGKGGAKRHRK. The sequence of the NH_2-terminal 11 aa peptide of histone H4, H4(1−11), is Ac-SGRGKGGKGLG. The sequence of the GAR peptide, R4, is Ac-GGRGGFGGRGGKGGRGGFGGRGGFG. The underlined Rs designate the methylation sites. The NH_2-terminal tail 31 aa peptide of human H3, H3(1−31), was synthesized and used as a substrate in CARM1 and PRMT6 analyses. The sequence of H4(1−20)FL is Ac-SGRGKGGKGDpr(FL)GKGGAKRHRK. Dpr stands for 2,3-diaminopropionic acid. The sequence of R4FL is Ac-GGRGGFGGRGGK(FL)GGRGGFGGRGGFG. In both cases, the fluorescein (FL) is attached to the side chain amino group.

Protein Expression and Purification. His6x-tagged PRMT1 was expressed from the pET28b vector. GST-PRMT1 is expressed from the pGEX-4T1 vector. His6x-tagged PRMT3 was expressed from the pReceiver vector. GST-mCARM1 was expressed from the pGEX-4T1 vector. His6x-tagged PRMT6 was expressed from the pET28a vector. All of the proteins were expressed in *Escherichia coli* BL21(DE3). All of the His6x-tagged proteins were purified on Ni-NTA beads, and the GST-tagged proteins were purified on glutathione agarose beads. Protein concentrations were determined using Bradford assay.

Virtual Screening. The virtual screening was conducted on a 40-node Linux cluster at Georgia State University using the same protocol as described before.[67,68] The 2D structures of ChemBridge database (about 0.4 million compounds) were first converted into 3D structures by using the CONCORD program.[39] Hydrogen atoms were then added to the 3D ligand structures, and all atoms were assigned with AM1-BCC partial charges[69−71] by the QuACPAC 1.1 software.[72] These structures were first examined based on a druglike property by the FILTER 2.0.1 software.[73] Before docking-based virtual screening, the PRMT1 structure (PDB entry: 1OR8) was added with hydrogen atoms and assigned with Kollman-all charges by the SYBYL 7.1 program.[74] Residues including Arg 3, Arg 9, Arg 15, Ile 44, His 45, Met 48, Leu 49, Arg 54, Thr 55, Asp 76, Val 77, Gly 78, Ser 79, Gly 80, Thr 81, Gly 82, Ile 83, Leu 84, Ile 99, Glu 100, Cys 101, Ser 102, Ile 104, Gly 126, Lys 127, Val 128, Glu 129, Ser 143, Glu 144, Met 155, and Thr 158 were defined as the active site to construct a grid for the structure-based virtual screening (Figure SI-6 in the Supporting Information). The position and conformation of each compound were optimized first by the anchor fragment orientation and then by the torsion minimization method implemented in the DOCK 6 program.[40] Fifty conformations and a maximum of 100 anchor orientations for each compound were generated, and all of the docked conformations were energy minimized by 100 iterations following procedures as described in literature.[40] The docked molecules were ranked based on the sum of the van der Waals and electrostatic energies implemented in the DOCK 6 program to obtain the top 1000 compounds. After the top hits were collected, the consensus scoring evaluation,[75] including ChemScore,[76,77] PLP,[78] ScreenScore,[79] ChemGauss, and ShapeGauss[80] implemented in the FRED 2.2.3 program, was processed,[73] as well as

hydrogen bond and hydrophobic profiles by the IDEA 8.8 software.[81] As the final step, a manual binding orientation and conformational examination were performed to harvest the final 50 hits for biochemical evaluation.

Radioactive Methylation Assay. The inhibitory activities of small molecule compounds were tested using carbon 14-labeled radioactive methylation assays. The assays were carried out in 0.6 mL plastic tubes at 30 °C in a reaction volume of 30 μL. The reaction buffer contained 50 mM HEPES (pH 8.0), 0.5 mM dithiothreitol (DTT), 1 mM EDTA, and 50 mM NaCl. In a typical procedure, 2 μM peptide substrate, 5 μM [^{14}C]-AdoMet, and varied concentrations of an inhibitor were preincubated in the reaction buffer for 5 min prior to the initiation by the addition of PRMT1 (0.1 μM final). After it was incubated for an appropriate period of time, the reaction was quenched by spreading the reaction mixture onto P81 filter paper discs (Whatman). The paper disk was washed with 1 L of 50 mM $NaHCO_3$, and dried in air for 2 h. The amount of methylated products was quantified by liquid scintillation. The IC_{50} value is the concentration of inhibitor at which half of the maximal activity is reached. The K_i for stilbamidine was calculated from IC_{50} by using the equation: $K_i = IC_{50}/(1 + [S]/K_m)$. K_m was obtained by measuring the initial velocity of reaction at different concentrations of a particular substrate and fitting the kinetic data with the Michaelis−Menten equation. The inhibition patterns of **3** and **6** were determined by measuring initial velocities of PRMT1 at a range of varied concentrations of one substrate, a fixed concentration of the other substrate, and selected concentrations of the inhibitors. The data were displayed in double reciprocal formats and fitted to competitive or noncompetitive kinetic equations.[82]

Inhibition of p300 Catalysis. Recombinant p300 HAT domain (1287−1666) was a gift from Dr. Philip Cole at Johns Hopkins University, and its expression was described in an earlier report.[83] The enzymatic activity of p300 and its inhibition by **3** and other compounds were measured by radioactive acetylation assays. A reaction mixture of 10 μM H4(1−20), 10 μM [^{14}C]-acetyl CoA, 20 nM p300, and increasing concentrations of the inhibitors were incubated in the reaction buffer [50 mM HEPES (pH 8.0), 50 mM NaCl, 0.5 mM DTT, and 1 mM EDTA] at 30 °C for 10 min, and the reaction was quenched by loading the mixture onto p81 filter paper. The radioactive products were quantified by liquid scintillation, and the fractional activity of p300 was plotted with respect to the concentration of individual inhibitors.

Fluorescent Binding Assay. The fluorescence intensity and anisotropy of fluorescein-labeled peptides were measured on a Fluoromax-4 spectrofluorometer (Horiba Jobin Yvon). The buffer was the same as that for the radioactive assay. The excitation wavelength and emission wavelength were selected at 498 and 524 nm, respectively. The competitive binding of small molecule compounds to the PRMT1−substrate solution was measured using the fluorescence anisotropy mode in similar manners as described previously.[41] Typically, 0.2 μM H4(1−20)FL and 2 μM PRMT1 were mixed, and increasing concentrations of an inhibitor were added until the fluorescence anisotropy signals leveled off. The anisotropy values at 524 nm from several scans were plotted as a function of inhibitor concentration. Data were fitted with a competitive binding model using DynaFit program to calculate the K_i value.[42,84] Also, fluorescence intensity changes of H4(1−20)FL at different concentrations of **3** were measured to detect their interaction. A 0.2 μM concentration of H4(1−20)FL at 30 °C was titrated with increasing concentrations of **3** (0−28.2 μM). NHS-fluorescein was used as a control. The fluorescence intensities of both H4(1−20)FL and NHS-fluorescein were corrected to remove the inner filter effect that was caused by **3** absorption, and the data were plotted as a function of the concentration of **3**. Job's method was applied to determine the binding stoichiometry of **3** with H4(1−20)FL. A series of solutions with a fixed total amount (0.225 nmol) but varied ratios (0−9) of **3** and H4-(1−20)FL in the same reaction buffer were prepared. The fluorescence intensity of each sample at 524 nm was measured, which is related to the amount of binding complex. The fluorescence intensity was divided by the molar fraction of H4-(1−20)FL and then plotted as a function of the molar fraction of **3**.

UV−Vis Spectroscopy of 3 upon Titration with H4(1−20) or PRMT1. The UV−vis spectra of compound **3** (40 μM in the same reaction buffer) were acquired on a Shimadzu UV-1700 spectrophotometer, in the presence of different concentrations of H4−20 or PRMT1.

CD Measurement. CD spectral changes of H4(1−20) upon the addition of different concentrations of **3** were measured on a Jasco J-810 spectropolarimeter. A 100 μM concentration of H4(1−20) was titrated with 0, 100, and 200 μM **3** in 10 mM Tris buffer (pH 7.4) in a 400 μL CD cuvette. The CD spectrum of each equilibrated sample was scanned (100 nm/min) with an accumulation of three times (Figure SI-5 in the Supporting Information).

Acknowledgment. Financial support from the American Heart Association, Georgia Cancer Coalition Distinguished Cancer Scholar Program, and the GSU Molecular Basis of Disease program are gratefully acknowledged. We thank Dr. Mark Bedford and Dr. Adam Frankel for providing the GST-PRMT1 and His6x-PRMT6 plasmids. We also thank Chao Yang for preparing PRMT3 and PRMT6 proteins and Dr. Siming Wang and Yanyi Chen for technical assistance with MALDI-MS.

Supporting Information Available: Additional structures, experimental data, figures, and graphs. This material is available free of charge via the Internet at http://pubs.acs.org.

References

(1) Pal, S.; Sif, S. Interplay between chromatin remodelers and protein arginine methyltransferases. *J. Cell. Physiol.* **2007**, *213*, 306–315.
(2) Lee, D. Y.; Teyssier, C.; Strahl, B. D.; Stallcup, M. R. Role of protein methylation in regulation of transcription. *Endocr. Rev.* **2005**, *26*, 147–170.
(3) Krause, C. D.; Yang, Z. H.; Kim, Y. S.; Lee, J. H.; Cook, J. R.; Pestka, S. Protein arginine methyltransferases: Evolution and assessment of their pharmacological and therapeutic potential. *Pharmacol. Ther.* **2007**, *113*, 50–87.
(4) Gary, J. D.; Clarke, S. RNA and protein interactions modulated by protein arginine methylation. *Prog. Nucleic Acid Res. Mol. Biol.* **1998**, *61*, 65–131.
(5) Boisvert, F. M.; Cote, J.; Boulanger, M. C.; Richard, S. A proteomic analysis of arginine-methylated protein complexes. *Mol. Cell. Proteomics* **2003**, *2*, 1319–1330.
(6) Bedford, M. T.; Richard, S. Arginine methylation an emerging regulator of protein function. *Mol. Cell* **2005**, *18*, 263–272.
(7) McBride, A. E.; Silver, P. A. State of the arg: Protein methylation at arginine comes of age. *Cell* **2001**, *106*, 5–8.
(8) Lee, J. H.; Cook, J. R.; Yang, Z. H.; Mirochnitchenko, O.; Gunderson, S. I.; Felix, A. M.; Herth, N.; Hoffmann, R.; Pestka, S. PRMT7, a new protein arginine methyltransferase that synthesizes symmetric dimethylarginine. *J. Biol. Chem.* **2005**, *280*, 3656–3664.
(9) Zhang, Y.; Reinberg, D. Transcription regulation by histone methylation: Interplay between different covalent modifications of the core histone tails. *Genes Dev.* **2001**, *15*, 2343–2360.
(10) Clarke, S. Protein methylation. *Curr. Opin. Cell Biol.* **1993**, *5*, 977–983.
(11) Bedford, M. T.; Clarke, S. G. Protein arginine methylation in mammals: Who, what, and why. *Mol. Cell* **2009**, *33*, 1–13.
(12) Scorilas, A.; Black, M. H.; Talieri, M.; Diamandis, E. P. Genomic organization, physical mapping, and expression analysis of the human protein arginine methyltransferase 1 gene. *Biochem. Biophys. Res. Commun.* **2000**, *278*, 349–359.
(13) Goulet, I.; Gauvin, G.; Boisvenue, S.; Cote, J. Alternative splicing yields protein arginine methyltransferase 1 isoforms with distinct activity, substrate specificity, and subcellular localization. *J. Biol. Chem.* **2007**, *282*, 33009–33021.

(14) Mathioudaki, K.; Papadokostopoulou, A.; Scorilas, A.; Xynopoulos, D.; Agnanti, N.; Talieri, M. The PRMT1 gene expression pattern in colon cancer. *Br. J. Cancer* **2008**, *99*, 2094–2099.
(15) Papadokostopoulou, A.; Mathioudaki, K.; Scorilas, A.; Xynopoulos, D.; Ardavanis, A.; Kouroumalis, E.; Talieri, M. Colon cancer and protein arginine methyltransferase 1 gene expression. *Anticancer Res.* **2009**, *29*, 1361–1366.
(16) Seligson, D. B.; Horvath, S.; Shi, T.; Yu, H.; Tze, S.; Grunstein, M.; Kurdistani, S. K. Global histone modification patterns predict risk of prostate cancer recurrence. *Nature* **2005**, *435*, 1262–1266.
(17) Cheung, N.; Chan, L. C.; Thompson, A.; Cleary, M. L.; So, C. W. Protein arginine-methyltransferase-dependent oncogenesis. *Nat. Cell Biol.* **2007**, *9*, 1208–1215.
(18) Hong, H.; Kao, C.; Jeng, M. H.; Eble, J. N.; Koch, M. O.; Gardner, T. A.; Zhang, S.; Li, L.; Pan, C. X.; Hu, Z.; MacLennan, G. T.; Cheng, L. Aberrant expression of CARM1, a transcriptional coactivator of androgen receptor, in the development of prostate carcinoma and androgen-independent status. *Cancer* **2004**, *101*, 83–89.
(19) Majumder, S.; Liu, Y.; Ford, O. H., 3rd; Mohler, J. L.; Whang, Y. E. Involvement of arginine methyltransferase CARM1 in androgen receptor function and prostate cancer cell viability. *Prostate* **2006**, *66*, 1292–1301.
(20) Wang, L.; Pal, S.; Sif, S. Protein arginine methyltransferase 5 suppresses the transcription of the RB family of tumor suppressors in leukemia and lymphoma cells. *Mol. Cell. Biol.* **2008**, *28*, 6262–6277.
(21) Kim, J. M.; Sohn, H. Y.; Yoon, S. Y.; Oh, J. H.; Yang, J. O.; Kim, J. H.; Song, K. S.; Rho, S. M.; Yoo, H. S.; Kim, Y. S.; Kim, J. G.; Kim, N. S. Identification of gastric cancer-related genes using a cDNA microarray containing novel expressed sequence tags expressed in gastric cancer cells. *Clin. Cancer Res.* **2005**, *11*, 473–482.
(22) Pal, S.; Vishwanath, S. N.; Erdjument-Bromage, H.; Tempst, P.; Sif, S. Human SWI/SNF-associated PRMT5 methylates histone H3 arginine 8 and negatively regulates expression of ST7 and NM23 tumor suppressor genes. *Mol. Cell. Biol.* **2004**, *24*, 9630–9645.
(23) Yildirim, A. O.; Bulau, P.; Zakrzewicz, D.; Kitowska, K. E.; Weissmann, N.; Grimminger, F.; Morty, R. E.; Eickelberg, O. Increased protein arginine methylation in chronic hypoxia: role of protein arginine methyltransferases. *Am. J. Respir. Cell Mol. Biol.* **2006**, *35*, 436–443.
(24) Maas, R. Pharmacotherapies and their influence on asymmetric dimethylargine (ADMA). *Vasc. Med.* **2005**, *10* (Suppl. 1), S49–S57.
(25) McKinsey, T. A.; Zhang, C. L.; Olson, E. N. Signaling chromatin to make muscle. *Curr. Opin. Cell Biol.* **2002**, *14*, 763–772.
(26) Spannhoff, A.; Sippl, W.; Jung, M. Cancer treatment of the future: Inhibitors of histone methyltransferases. *Int. J. Biochem. Cell Biol.* **2009**, *41*, 4–11.
(27) Zheng, Y. G.; Wu, J.; Chen, Z.; Goodman, M. Chemical regulation of epigenetic modifications: Opportunities for new cancer therapy. *Med. Res. Rev.* **2008**, *28*, 645–687.
(28) Mai, A.; Altucci, L. Epi-drugs to fight cancer: From chemistry to cancer treatment, the road ahead. *Int. J. Biochem. Cell Biol.* **2009**, *41*, 199–213.
(29) Cheng, D.; Yadav, N.; King, R. W.; Swanson, M. S.; Weinstein, E. J.; Bedford, M. T. Small molecule regulators of protein arginine methyltransferases. *J. Biol. Chem.* **2004**, *279*, 23892–23899.
(30) Spannhoff, A.; Heinke, R.; Bauer, I.; Trojer, P.; Metzger, E.; Gust, R.; Schule, R.; Brosch, G.; Sippl, W.; Jung, M. Target-based approach to inhibitors of histone arginine methyltransferases. *J. Med. Chem.* **2007**, *50*, 2319–2325.
(31) Spannhoff, A.; Machmur, R.; Heinke, R.; Trojer, P.; Bauer, I.; Brosch, G.; Schule, R.; Hanefeld, W.; Sippl, W.; Jung, M. A novel arginine methyltransferase inhibitor with cellular activity. *Bioorg. Med. Chem. Lett.* **2007**, *17*, 4150–4153.
(32) Purandare, A. V.; Chen, Z.; Huynh, T.; Pang, S.; Geng, J.; Vaccaro, W.; Poss, M. A.; Oconnell, J.; Nowak, K.; Jayaraman, L. Pyrazole inhibitors of coactivator associated arginine methyltransferase 1 (CARM1). *Bioorg. Med. Chem. Lett.* **2008**, *18*, 4438–4441.
(33) Heinke, R.; Spannhoff, A.; Meier, R.; Trojer, P.; Bauer, I.; Jung, M.; Sippl, W. Virtual screening and biological characterization of novel histone arginine methyltransferase PRMT1 inhibitors. *ChemMedChem* **2009**, *4*, 69–77.
(34) Mai, A.; Cheng, D.; Bedford, M. T.; Valente, S.; Nebbioso, A.; Perrone, A.; Brosch, G.; Sbardella, G.; De Bellis, F.; Miceli, M.; Altucci, L. Epigenetic Multiple Ligands: Mixed Histone/Protein Methyltransferase, Acetyltransferase, and Class III Deacetylase (Sirtuin) Inhibitors. *J. Med. Chem.* **2008**, *51*, 2279–2290.
(35) Ragno, R.; Simeoni, S.; Castellano, S.; Vicidomini, C.; Mai, A.; Caroli, A.; Tramontano, A.; Bonaccini, C.; Trojer, P.; Bauer, I.; Brosch, G.; Sbardella, G. Small molecule inhibitors of histone arginine methyltransferases: Homology modeling, molecular docking, binding mode analysis, and biological evaluations. *J. Med. Chem.* **2007**, *50*, 1241–1253.
(36) Mai, A.; Valente, S.; Cheng, D.; Perrone, A.; Ragno, R.; Simeoni, S.; Sbardella, G.; Brosch, G.; Nebbioso, A.; Conte, M.; Altucci, L.; Bedford, M. T. Synthesis and biological validation of novel synthetic histone/protein methyltransferase inhibitors. *ChemMedChem* **2007**, *2*, 987–991.
(37) Osborne, T.; Roska, R. L.; Rajski, S. R.; Thompson, P. R. In Situ Generation of a Bisubstrate Analogue for Protein Arginine Methyltransferase 1. *J. Am. Chem. Soc.* **2008**, *130*, 4574–4575.
(38) Zhang, X.; Cheng, X. Structure of the predominant protein arginine methyltransferase PRMT1 and analysis of its binding to substrate peptides. *Structure* **2003**, *11*, 509–520.
(39) Pearlman, R. S. CONCORD: Rapid Generation of High Quality Approximate 3D Molecular Structures. *Chem. Des. Autom. News* **1987**, *2*, 1–7.
(40) Moustakas, D. T.; Lang, P. T.; Pegg, S.; Pettersen, E.; Kuntz, I. D.; Brooijmans, N.; Rizzo, R. C. Development and Validation of a Modular, Extensible Docking Program: DOCK 5. *J. Comput.-Aided Mol. Des.* **2006**, *20*, 601–619.
(41) Feng, Y.; Xie, N.; Wu, J.; Yang, C.; Zheng, Y. G. Inhibitory study of protein arginine methyltransferase 1 using a fluorescent approach. *Biochem. Biophys. Res. Commun.* **2009**, *379*, 567–572.
(42) Kuzmic, P. Program DYNAFIT for the analysis of enzyme kinetic data: application to HIV proteinase. *Anal. Biochem.* **1996**, *237*, 260–273.
(43) Segel, I. H. *Enzyme Kinetics: Behavior and Analysis of Rapid Equilibrium and Steady State Enzyme Systems*; Wiley: New York, 1975; p xxii, 957 pp.
(44) Thompson, P. R.; Kurooka, H.; Nakatani, Y.; Cole, P. A. Transcriptional coactivator protein p300. Kinetic characterization of its histone acetyltransferase activity. *J. Biol. Chem.* **2001**, *276*, 33721–33729.
(45) Utley, R. T.; Lacoste, N.; Jobin-Robitaille, O.; Allard, S.; Cote, J. Regulation of NuA4 histone acetyltransferase activity in transcription and DNA repair by phosphorylation of histone H4. *Mol. Cell. Biol.* **2005**, *25*, 8179–8190.
(46) Cheung, W. L.; Turner, F. B.; Krishnamoorthy, T.; Wolner, B.; Ahn, S. H.; Foley, M.; Dorsey, J. A.; Peterson, C. L.; Berger, S. L.; Allis, C. D. Phosphorylation of histone H4 serine 1 during DNA damage requires casein kinase II in S. cerevisiae. *Curr. Biol.* **2005**, *15*, 656–660.
(47) Wang, H.; Huang, Z. Q.; Xia, L.; Feng, Q.; Erdjument-Bromage, H.; Strahl, B. D.; Briggs, S. D.; Allis, C. D.; Wong, J.; Tempst, P.; Zhang, Y. Methylation of histone H4 at arginine 3 facilitating transcriptional activation by nuclear hormone receptor. *Science* **2001**, *293*, 853–857.
(48) Schiltz, R. L.; Mizzen, C. A.; Vassilev, A.; Cook, R. G.; Allis, C. D.; Nakatani, Y. Overlapping but distinct patterns of histone acetylation by the human coactivators p300 and PCAF within nucleosomal substrates. *J. Biol. Chem.* **1999**, *274*, 1189–1192.
(49) Ogryzko, V. V.; Schiltz, R. L.; Russanova, V.; Howard, B. H.; Nakatani, Y. The transcriptional coactivators p300 and CBP are histone acetyltransferases. *Cell* **1996**, *87*, 953–959.
(50) Smith, E. R.; Eisen, A.; Gu, W.; Sattah, M.; Pannuti, A.; Zhou, J.; Cook, R. G.; Lucchesi, J. C.; Allis, C. D. ESA1 is a histone acetyltransferase that is essential for growth in yeast. *Proc. Natl. Acad. Sci. U.S.A.* **1998**, *95*, 3561–3565.
(51) Kimura, A.; Horikoshi, M. Tip60 acetylates six lysines of a specific class in core histones in vitro. *Genes Cells* **1998**, *3*, 789–800.
(52) Zhang, K.; Williams, K. E.; Huang, L.; Yau, P.; Siino, J. S.; Bradbury, E. M.; Jones, P. R.; Minch, M. J.; Burlingame, A. L. Histone acetylation and deacetylation: Identification of acetylation and methylation sites of HeLa histone H4 by mass spectrometry. *Mol. Cell Proteomics* **2002**, *1*, 500–508.
(53) Zhang, L.; Eugeni, E. E.; Parthun, M. R.; Freitas, M. A. Identification of novel histone post-translational modifications by peptide mass fingerprinting. *Chromosoma* **2003**, *112*, 77–86.
(54) Schotta, G.; Lachner, M.; Sarma, K.; Ebert, A.; Sengupta, R.; Reuter, G.; Reinberg, D.; Jenuwein, T. A silencing pathway to induce H3-K9 and H4-K20 trimethylation at constitutive heterochromatin. *Genes Dev.* **2004**, *18*, 1251–1262.
(55) Beck, H. C.; Nielsen, E. C.; Matthiesen, R.; Jensen, L. H.; Sehested, M.; Finn, P.; Grauslund, M.; Hansen, A. M.; Jensen, O. N. Quantitative proteomic analysis of post-translational modifications of human histones. *Mol. Cell Proteomics* **2006**, *5*, 1314–1325.
(56) Selvi, B. R.; Batta, K.; Kishore, A. H.; Mantelingu, K.; Varier, R. A.; Balasubramanyam, K.; Pradhan, S. K.; Dasgupta, D.; Sriram, S.; Agrawal, S.; Kundu, T. K. Identification of a novel inhibitor of coactivator-associated arginine methyltransferase 1

(CARM1)-mediated methylation of histone H3 Arg-17. *J. Biol. Chem.* **2010**, *285*, 7143–7152.
(57) Skillman, A. G.; Maurer, K. W.; Roe, D. C.; Stauber, M. J.; Eargle, D.; Ewing, T. J.; Muscate, A.; Davioud-Charvet, E.; Medaglia, M. V.; Fisher, R. J.; Arnold, E.; Gao, H. Q.; Buckheit, R.; Boyer, P. L.; Hughes, S. H.; Kuntz, I. D.; Kenyon, G. L. A novel mechanism for inhibition of HIV-1 reverse transcriptase. *Bioorg. Chem.* **2002**, *30*, 443–458.
(58) McGeary, R. P.; Bennett, A. J.; Tran, Q. B.; Cosgrove, K. L.; Ross, B. P. Suramin: Clinical uses and structure-activity relationships. *Mini Rev. Med. Chem.* **2008**, *8*, 1384–1394.
(59) La Rocca, R. V.; Stein, C. A.; Danesi, R.; Myers, C. E. Suramin, a novel antitumor compound. *J. Steroid Biochem. Mol. Biol.* **1990**, *37*, 893–898.
(60) Lima, L. M.; Becker, C. F.; Giesel, G. M.; Marques, A. F.; Cargnelutti, M. T.; de Oliveira Neto, M.; Monteiro, R. Q.; Verli, H.; Polikarpov, I. Structural and thermodynamic analysis of thrombin:suramin interaction in solution and crystal phases. *Biochim. Biophys. Acta* **2009**, *1794*, 873–881.
(61) Ganesh, V. K.; Muthuvel, S. K.; Smith, S. A.; Kotwal, G. J.; Murthy, K. H. Structural basis for antagonism by suramin of heparin binding to vaccinia complement protein. *Biochemistry* **2005**, *44*, 10757–10765.
(62) Schuetz, A.; Min, J.; Antoshenko, T.; Wang, C. L.; Allali-Hassani, A.; Dong, A.; Loppnau, P.; Vedadi, M.; Bochkarev, A.; Sternglanz, R.; Plotnikov, A. N. Structural basis of inhibition of the human NAD+-dependent deacetylase SIRT5 by suramin. *Structure* **2007**, *15*, 377–389.
(63) Fujiuchi, S.; Ohsaki, Y.; Kikuchi, K. Suramin inhibits the growth of non-small-cell lung cancer cells that express the epidermal growth factor receptor. *Oncology* **1997**, *54*, 134–140.
(64) Kathir, K. M.; Kumar, T. K.; Yu, C. Understanding the mechanism of the antimitogenic activity of suramin. *Biochemistry* **2006**, *45*, 899–906.
(65) Sun, Y.; Jiang, X.; Chen, S.; Price, B. D. Inhibition of histone acetyltransferase activity by anacardic acid sensitizes tumor cells to ionizing radiation. *FEBS Lett.* **2006**, *580*, 4353–4356.
(66) Xie, N.; Elangwe, E. N.; Asher, S.; Zheng, Y. G. A dual-mode fluorescence strategy for screening HAT modulators. *Bioconjugate Chem.* **2009**, *20*, 360–366.
(67) Li, M. Y.; Huang, Y. J.; Tai, P. C.; Wang, B. H. Discovery of the first SecA inhibitors using structure-based virtual screening. *Biochem. Biophys. Res. Commun.* **2008**, *368*, 839–845.
(68) Li, M. Y.; Ni, N. T.; Chou, H. T.; Lu, C. D.; Tai, P. C.; Wang, B. H. Structure-based discovery and experimental verification of novel Al-2 quorum sensing inhibitors against Vibrio harveyi. *ChemMedChem* **2008**, *3*, 1242–1249.
(69) Jakalian, A.; Bush, B. L.; Jack, D. B.; Bayly, C. I. Fast, Efficient Generation of High-Quality Atomic Charges. AM1-BCC Model: I. Method. *J. Comput. Chem.* **2000**, *21*, 132–146.
(70) Jakalian, A.; Jack, D. B.; Bayly, C. I. Fast, Efficient Generation of High-Quality Atomic Charges. AM1-BCC Model: II. Parameterization and Validation. *J. Comput. Chem.* **2002**, *23*, 1623–1641.
(71) Tsai, K. C.; Wang, S. H.; Hsiao, N. W.; Li, M. Y.; Wang, B. H. The effect of different electrostatic potentials on docking accuracy: A case study using DOCK5.4. *Bioorg. Med. Chem. Lett.* **2008**, *18*, 3509–3512.
(72) *QuACPAC*, Release version 1.1; OpenEye Scientific Software, Inc.: Santa Fe, NM, **2007**.
(73) *FRED*, Release version 2.2.3; OpenEye Scientific Software, Inc.: Santa Fe, NM, **2007**.
(74) *SYBYL 7.1*; Tripos Inc.: St. Louis, MO, **2005**.
(75) Feher, M. Consensus scoring for protein-ligand interactions. *Drug Discovery Today* **2006**, *11*, 421–428.
(76) Eldridge, M. D.; Murray, C. W.; Auton, T. R.; Paolini, G. V.; Mee, R. P. Empirical scoring functions: I. The development of a fast empirical scoring function to estimate the binding affinity of ligands in receptor complexes. *J. Comput.-Aided Mol. Des.* **1997**, *11*, 425–445.
(77) Murray, C. W.; Auton, T. R.; Eldridge, M. D. Empirical scoring functions. II. The testing of an empirical scoring function for the prediction of ligand-receptor binding affinities and the use of Bayesian regression to improve the quality of the model. *J. Comput.-Aided Mol. Des.* **1998**, *12*, 503–519.
(78) Verkhivker, G. M.; Bouzida, D.; Gehlhaar, D. K.; Rejto, P. A.; Arthurs, S.; Colson, A. B.; Freer, S. T.; Larson, V.; Luty, B. A.; Marrone, T.; Rose, P. W. Deciphering common failures in molecular docking of ligand-protein complexes. *J. Comput.-Aided Mol. Des.* **2000**, *14*, 731–751.
(79) Stahl, M.; Rarey, M. Detailed analysis of scoring functions for virtual screening. *J. Med. Chem.* **2001**, *44*, 1035–1042.
(80) McGann, M. R.; Almond, H. R.; Nicholls, A.; Grant, J. A.; Brown, F. K. Gaussian docking functions. *Biopolymers* **2003**, *68*, 76–90.
(81) *IDEA*, Version 8.8; Breadth Technology: Taipei, Taiwan, 2007.
(82) Wu, J.; Xie, N.; Wu, Z.; Zhang, Y.; Zheng, Y. G. Bisubstrate Inhibitors of the MYST HATs Esa1 and Tip60. *Bioorg. Med. Chem.* **2009**, *17*, 1381–1386.
(83) Thompson, P. R.; Wang, D.; Wang, L.; Fulco, M.; Pediconi, N.; Zhang, D.; An, W.; Ge, Q.; Roeder, R. G.; Wong, J.; Levrero, M.; Sartorelli, V.; Cotter, R. J.; Cole, P. A. Regulation of the p300 HAT domain via a novel activation loop. *Nat. Struct. Mol. Biol.* **2004**, *11*, 308–315.
(84) Kuzmic, P. A generalized numerical approach to rapid-equilibrium enzyme kinetics: Application to 17beta-HSD. *Mol. Cell. Endocrinol.* **2006**, *248*, 172–181.